MELISSA observations of F-region irregularities

G. K. Zewdie[1], F. S. Rodrigues[1], and E. R. de Paula[2]

Abstract. The Measurements of Equatorial and Low-latitude Ionospheric irregularities over Sao Luis, South America (MELISSA) system is a newly developed 30 MHz coherent backscatter radar interferometer deployed in Sao Luis, Brazil (2.59° S, 44.21° N, -3.99° dip lat) near the magnetic equator. Here, we present the first results of our analysis of equatorial spread F (ESF) observations made by the system. We found that the system was capable of detecting bottom-type, bottomside and topside scattering structures. We also determined spectral characteristics of the 30 MHz echoes observed during typical ESF events. Previous studies found supersonic, overspread echoes at 50 MHz and underspread echoes with smaller mean Doppler velocities at 18 MHz. Analyses of the first observations show that the mean Doppler velocities of the echoes observed by MELISSA are, mostly, within ±100 m/s. We also found that the spectral widths are, in general, between 25 and 75 m/s. The largest Doppler velocities and spectral widths are observed during the passage of topside scattering structures. The spectral characteristics are signatures of the early stage, turbulent evolution of radar plumes. Bottomside and bottom-type echoes show narrow spectral widths and reduced mean Doppler velocities. Our results motivate more comprehensive analyses of the spectral characteristics of the echoes observed by MELISSA and their interpretation

1. Introduction

A number of unique and intriguing ionospheric phenomena are known to occur in the magnetic equatorial region. Among these, are the so-called equatorial spread F (ESF) events. ESF is a general (and historical) name given to signatures of irregularities in the ionospheric electron density observed by a number of different instruments [e.g. *Booker and Wells*, 1938; *Woodman*, 2009]. The scale size of the ESF irregularities can vary from centimeters to hundreds of kilometers [*Kelley*, 1985]. ESF is also known to extend from the bottomside F region to the topside, reaching heights above a thousand kilometers [e.g, *Hysell*, 2000]. In large scale ESF perturbations, the plasma density has been found to be lower than the background plasma by a few orders of magnitude [e.g. *Hanson and Sanatani*, 1973].

In general, ESF irregularities are observed to develop in the bottomside F-region at the geomagnetic equator, within 1-2 hours after sunset. Then, ESF irregularities reach higher altitudes, extend along magnetic field lines and are observed at off-equatorial latitudes. In exceptional occasions, ESF has been observed to start after midnight and during daytime hours [*Chau and Woodman*, 2001]. We currently seek a better understanding of the ESF morphology and day-to-day variability.

ESF studies are also motivated by its impact on the propagation of radio waves used for navigation, communication and remote sensing. Electron density irregularities cause spatial and temporal changes in the index of refraction of the ionospheric propagation channel [e.g, *Kintner et al.*, 2007].

ESF irregularities have been studied for tens of years using ground- and space-based instruments [e.g. *Hysell and Burcham*, 1998; *McClure et al.*, 1977]. Incoherent and coherent radar observations made at the Jicamarca Radio Observatory (JRO), a magnetic equatorial site located near Lima in Peru, have been particularly important. The Jicamarca radar observations have allowed to investigate the vertical extent of 3-meter scale size ESF irregularities, their temporal variability, their seasonal (in the Peruvian sector) and solar flux variability, and even their spatial distribution in the magnetic equatorial plane [e.g. *Hysell and Woodman*, 1997]. The advances made by Jicamarca inspired the installation of other radar systems at different longitude sectors [e.g. *de Paula and Hysell*, 2004; *Tiwari et al.*, 2004; *Otsuka et al.*, 2009; *Ning et al.*, 2012].

de Paula and Hysell [2004], in particular, describes a low-power 30 MHz coherent backscatter radar system deployed at the magnetic equatorial site of Sao Luis, Brazil in 2000. The location of the site has a number of interesting features. For instance, it is located on the east side of the South American sector, and allows joint studies across the continent with Jicamarca. The Sao Luis site is also conveniently located near both the magnetic and geographic equator. Finally, the site is also located in a region of large magnetic declination. Due to a number of technical problems, the Sao Luis radar (also referred to as the FCI radar) stopped working in 2012. In order to continue observations in Sao Luis, a collaborative effort was initiated, which allowed the design, development and deployment of a new system.

This paper describes the results of our analyses of the first observations of meter-scale F-region irregularities made with a new 30 MHz coherent backscatter radar interferometer deployed in Sao Luis. We focus, in particular, on the results of our analysis of the temporal and spatial variations of the intensity, mean Doppler velocity, and spectral widths of typical equatorial spread F events. Typical ESF events are those occurring in pre-midnight hours during regular ESF season in the Brazilian sector. That is, ESF events occurring between September and March of each year.

2. Instrumentation

In March 2014, we installed, tested and made the first F-region measurements with a newly developed 30 MHz coherent backscatter radar system. The Measurements of Low latitude and Equatorial Ionospheric irregularities over Sao Luis in South America (MELISSA) radar is an international

[1]William B. Hanson Center for Space Sciences, The University of Texas at Dallas, TX, USA

[2]Instituto Nacional de Pesquisas Espaciais, Sao José dos Campos, SP, Brazil

0148-02279.00

scientific collaboration between the University of Texas at Dallas (UTD), the Brazilian National Institute for Space Research (INPE) and the Jicamarca Radio Observatory (JRO) in Peru. The radar is installed in Sao Luis, Brazil (see Figure 1) where, previously, another 30 MHz radar operated between 2000 and 2012.

The system is formed by a digital data acquisition system, a radar controller, and a direct digital synthesizer (DDS) developed at Jicamarca. For transmission, we use a 16 kW peak power, dual output solid-state transmitter, which was designed and developed by ATRAD atmospheric radar systems. The transmitter operates at 29.795 MHz and has a 10% maximum duty cycle. Transmissions use the same antenna setup of the old Sao Luis radar. The setup is formed by four independent sets of antenna modules aligned in the zonal magnetic direction. Each antenna module is formed by a 4x4 array of Yagi antennas. The one-way half-power beam width (HPBW) of each antenna module is approximately 16° in both EW and NS direction. Two modules are used for transmission only, and all the modules are used for reception. The antenna modules are spaced non-uniformly in the magnetic zonal direction producing 7 non-redundant baselines that, in the future, will be used to obtain estimates of the spatial correlation of the backscatter on the ground (visibility estimates) [e.g. *Rodrigues et al.*, 2008]. Visibility estimates will be used in interferometric in-beam radar imaging studies. For this study and presentation, we used the measurements made by a single antenna module only, which allows us to make conventional radar observations. Results of interferometric observations will be reported in the future.

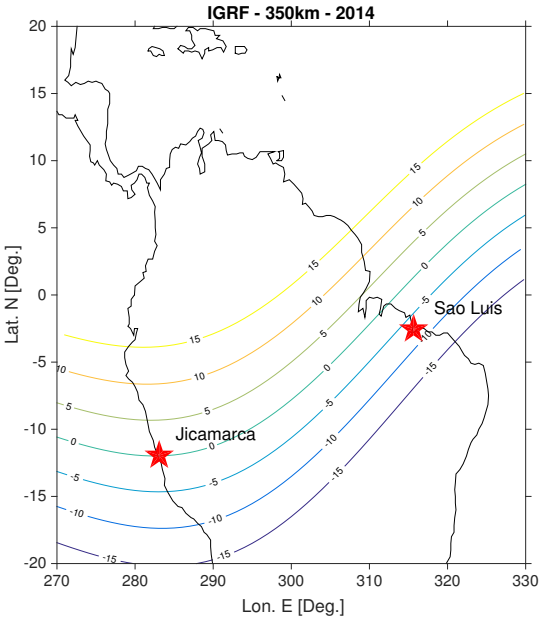

Figure 1. The location of the Sao Luis radar site in Brazil. The Jicamarca location is indicated for reference. Iso-countours of magnetic inclination are also shown. Magnetic values are from the International Geomagnetic Reference Field (IGRF) model for 2014.

3. Measurements and Analysis

3.1. Radar mode

F-region measurements have been made with 28-bit coded pulses. Each baud is 2.4 km long. The inter-pulse period (IPP) of the soundings is 1401.6 km, and the returns are sampled every 2.4 km (no oversampling). A total of 500 samples are obtained per IPP with the first sample from 90 km altitude. The measurements are made between approximately 18:00 LT and 08:00 LT of the following day. Measurements are not made on a daily basis at this point.

3.2. Observation Period

The observations used in this study were made between March and August 2014. This time window covers a period of low-to-moderate solar flux conditions with a mean F10.7 solar flux index of about 137 SFU. About 55 days of observations are available for this study. A number of observations were made in March and April when ESF occurrence starts to decrease in

the Eastern American sector. During that period we observed cases of well-developed ESF events producing topside echoing layers and then cases of weak ESF represented by bottomside and bottom-type echoing layers.

Table 1 summarizes the radar parameters used for F-region measurements and analysis parameters used for spectral estimation.

Table 1. Summary of parameters used in this experiment.

Parameter	Value
Peak TX Power	16 kW
Code	28 bit
Baud length	2.4 km
IPP	1401.6 km
Number of samples	500
Lowest height sampled	90 km
Coherent integration	None
Number of FFT points	64
Number of FFT spectra averaged	25

3.3. Analysis

For this study, we carried out conventional analysis of the measurements made by only one of the four sets of antennas of the system. We derived estimates of the signal-to-noise ratio (SNR) of the measured echoes, which are used to determine the temporal and spatial (height) variation of meter-scale irregularities associated with ESF. We also computed the first and second spectral moments of the echoes, which are commonly used as a proxy of the bulk velocity and turbulence strength of the scattering structure within the volume illuminated by the radar [e.g. *Hysell et al.*, 2004].

The moments were obtained from Doppler spectra, which were estimated using a Fast Fourier Transform (FFT) algorithm. No coherent integration of the measured voltages was used, which allowed us to obtain unaliased Doppler spectra with velocities between -267 m/s and +267 m/s. A total of 64 samples were used in the FFT, and a total of 25 spectra were averaged.

The mean Doppler velocity and spectral widths were obtained by fitting a Gaussian model to the measured spectra.

4. Results and Discussion

Figure 2 shows an example of our results. The top panel shows the Range-Time-Intensity (RTI) map of the echoes observed on March 22, 2014 when different types of F-region echoing regions were observed. Only measurements made between 19:00 and 24:00 LT are shown here. The RTI map shows the occurrence of a bottom-type layer between approximately 19:30 LT and 20:00 LT and around 400 km altitude. Around 19:40 LT the RTI map shows topside (above 600 km altitude) echoes indicating the detection of well-developed ESF event (plume). Echoes as strong as 15 dB were observed during the initial stage of the event and became weaker as time progressed. Only very weak echoes were observed by midnight. A second topside structure is observed around 21:00 LT with echoes reaching above 1000 km altitude.

The bottom panels show examples of the measured spectra for different times and heights. Columns (rows) correspond to different times (heights), which are indicated in each panel. The times/heights at which spectra were measured are also indicated (black boxes) in the RTI map. Note that spectra were arranged so that positive values represent downward velocities. The most striking feature of the measurements shown in Figure 2 is that the spectra, in most cases, are single-peaked and Gaussian shaped. We have, however, also found cases of skewed, and/or double peaked spectra at times. The spectra in the second column (for 20:07 LT) show examples of spectra that would not be well represented by a Gaussian function. A more comprehensive analyses of the shape of ESF spectra will be carried out in the future using multi-day observations.

The spectra also show relative large widths at 20:07 LT, and much narrower spectral widths in the other panels. This is a result of highly turbulent state of the ionospheric plasma around the passage of the plume seen around 20:00 LT.

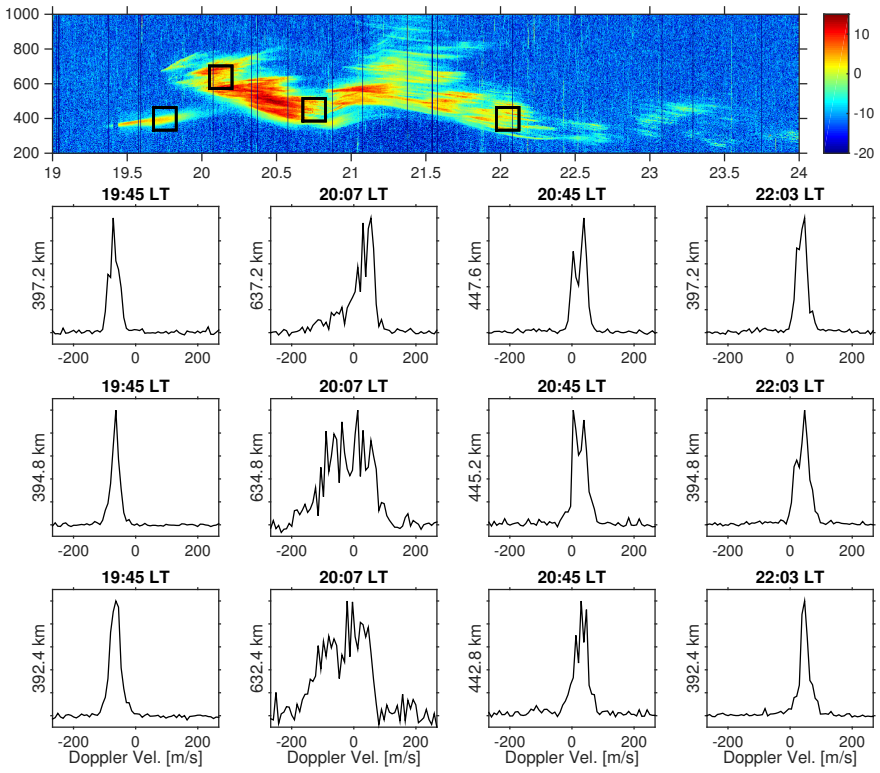

Figure 2. The top panel shows the RTI map of observations made by the MELISSA system on March 22, 2014. The bottom panels show examples of spectra estimated from observations made at different times and heights.

Figure 3 summarizes the single-antenna measurements made on March 22. The top panel shows, again, the RTI map. The middle panel shows the mean Doppler velocities estimated as a function of time and height. The bottom panel shows the estimated spectral widths. One can see that the velocities are, mostly, upward during the passage of the radar plumes, around 20:00 and 21:00 LT. The echoes associated with the plumes also have wide spectral widths.

The echoes associated with the bottom-type layer (19:00-21:30 LT) also show upward velocities. The spectra, however, show very narrow widths ($<$ 30 of m/s)

The bottomside echoes seen between plumes and later at night show downward velocities and narrow spectral widths.

The most striking feature of our observations is the fact that the velocities, in general, are well within $\pm$100 m/s at all times. Previous studies using the 50 MHz radar at the Jicamarca Radio Observatory indicated that echoes from active topside ESF echoes are overspread. This has led *Hysell et al.* [2004] to use advanced aperiodic pulse techniques to determine the ESF spectra. They found mean Doppler velocities reaching 400 - 600 m/s. *Tiwari et al.* [2004], on the other hand, analyzed the spectra of equatorial spread F echoes observed by a 18 MHz radar installed in Trivandrum near the magnetic equator in India between 2008 and 2010, a period of high solar flux activity. They found no evidence of supersonic velocities in their observations. The measurements also showed that the spectral widths were, in general, within 150 m/s.

4.1. Statistics of echo parameters

Figure 4 show histograms summarizing the distribution of spectral parameters estimated from the observations made on March 22. For the construction of the

histograms, we used only data from echoes with SNR $\geq$ 0 dB. We also only used spectral parameters obtained from fitting the Gaussian curve with reduced residuals.

The histograms confirm that the mean Doppler velocities are, mostly, within $\pm$ 100 m/s. The spectral widths are also well within 100 m/s. Most of the spectral widths are between 25 m/s and 75 m/s.

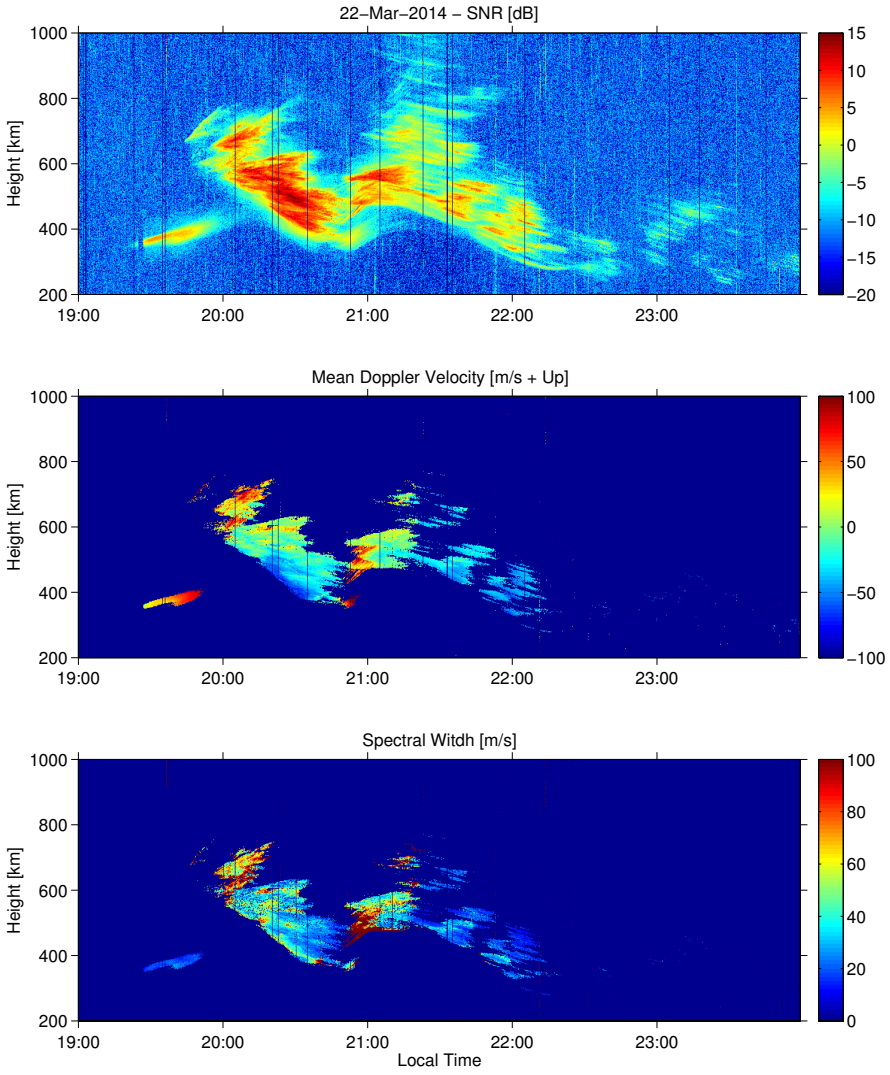

Figure 3. Example of parameters derived from conventional radar measurements made by MELISSA on March 22, 2014. The top panel shows the signal-to-noise ratio (SNR in dB) of the echoes. The middle panel shows the mean Doppler velocity (positive values represent upward velocities). The bottom panel shows the spectral widths.

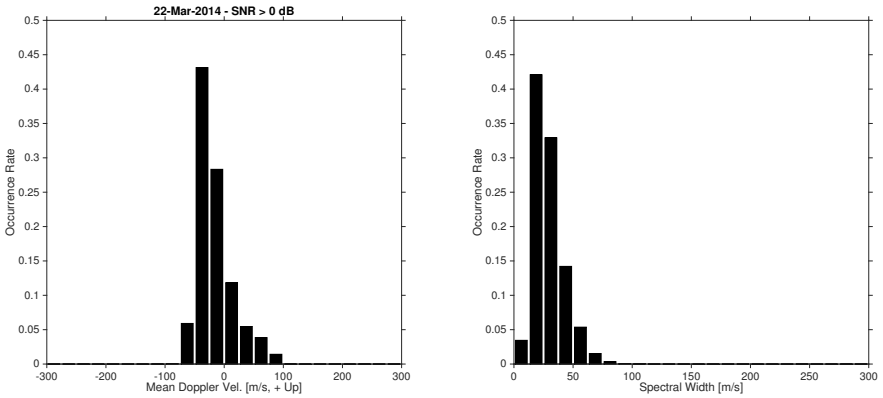

Figure 4. Histograms of mean Doppler velocities (+ Up) and spectral widths estimated from the observations made by MELISSA on March 22, 2014. Only parameters from relatively strong echoes (SNR $>$ 0 dB) and good fits (small residuals) were used to construct the histograms.

5. Concluding Remarks

We presented results of an spectral analysis of the first measurements of equatorial spread F made by the newly developed MELISSA radar system. The Measurements of Equatorial and Low-latitude Ionospheric irregularities over Sao Luis, South America (MELISSA) system is a 30 MHz coherent backscatter radar interferometer deployed in Sao Luis, Brazil (2.59° S, 44.21° N, -3.99° dip lat) near the magnetic equator. It replaces the FCI radar that operated in Sao Luis between 2000 and 2012. We found that the new system was capable of detecting bottom-type, bottomside and topside scattering structures.

Previous studies found supersonic, overspread echoes at 50 MHz and underspread echoes at 18 MHz [e.g. *Hysell et al.*, 2004; *Tiwari et al.*, 2004]. We found that the mean Doppler velocities of the echoes observed by MELISSA are, mostly, within ±100 m/s. We also found that the spectral widths are, in general, narrower than 100 m/s with greatest occurrences between 25 and 75 m/s.

The largest Doppler velocities and spectral widths are observed during the passage of topside scattering structures early at night. The spectral characteristics are signatures of turbulent flows within radar plumes.

Bottomside irregularities observed between plumes and later at night have narrow spectral widths ($\lesssim$ 30 m/s) and positive (downward) mean Doppler velocities, which can be representative of the background plasma drift conditions.

Acknowledgments. This work was supported by AFOSR (FA9550-13-1-0095). The authors would like to thank the technical staff from INPE and Jicamarca for helping deploying, testing, and maintaing the radar system.

References

Booker, H. G., and H. W. Wells (1938), Scattering of radio waves by the F-region of the ionosphere, *Terrestrial Magnetism and Atmospheric Electricity*, *43*(3), 249–256.

Chau, J. L., and R. F. Woodman (2001), Interferometric and dual beam observations of daytime spread-F-like irregularities over jicamarca, *Geophysical Research Letters*, *28*(18), 3581–3584, doi:10.1029/2001GL013404.

de Paula, E. R., and D. L. Hysell (2004), The São Luís 30 MHz coherent scatter ionospheric radar: System description and initial results, *Radio Sci.*, *39*, RS1014, doi: 10.1029/2003RS002914.

Hanson, W. B., and S. Sanatani (1973), Large Ni gradients below the equatorial F peak, *Journal of Geophysical Research*, *78*(7), 1167–1173, doi:10.1029/JA078i007p01167.

Hysell, D. (2000), An overview and synthesis of plasma irregularities in equatorial spread F, *Journal of Atmospheric and Solar-Terrestrial Physics*, *62*(12), 1037 – 1056, doi: http://dx.doi.org/10.1016/S1364-6826(00)00095-X.

Hysell, D. L., and J. D. Burcham (1998), Julia radar studies of equatorial spread F, *Journal of Geophysical Research: Space Physics*, *103*(A12), 29,155–29,167, doi:10.1029/98JA02655.

Hysell, D. L., and R. F. Woodman (1997), Imaging coherent backscatter radar observations of topside equatorial spread F, *Radio Science*, *32*(6), 2309–2320, doi:10.1029/97RS01802.

Hysell, D. L., J. Chun, and J. L. Chau (2004), Bottom-type scattering layers and equatorial spread F, *Annales Geophysicae*, *22*(12), 4061–4069, doi:10.5194/angeo-22-4061-2004.

Kelley, M. (1985), Equatorial spread-f: recent results and outstanding problems, *Journal of Atmospheric and Terrestrial Physics*, *47*(810), 745 – 752, doi: http://dx.doi.org/10.1016/0021-9169(85)90051-0.

Kintner, P. M., B. M. Ldevina, and E. R. de Paula (2007), GPS and ionospheric scintillations, *Space Weather*, *5*, doi: 10.1029/2006SW000260.

McClure, J. P., W. B. Hanson, and J. H. Hoffman (1977), Plasma bubbles and irregularities in the equatorial ionosphere, *Journal of Geophysical Research*, *82*(19), 2650–2656, doi: 10.1029/JA082i019p02650.

Ning, B., L. Hu, G. Li, L. Liu, and W. Wan (2012), The first time observations of low-latitude ionospheric irregularities by vhf radar in hainan, *Science China Technological Sciences*, *55*(5), 1189–1197, doi:10.1007/s11431-012-4800-2.

Otsuka, Y., T. Ogawa, and Effendy (2009), Vhf radar observations of nighttime F-region field-aligned irregularities over kototabang, indonesia, *Earth, Planets and Space*, *61*(4), 431–437, doi:10.1186/BF03353159.

Rodrigues, F. S., D. L. Hysell, and E. R. de Paula (2008), Coherent backscatter radar imaging in brazil: large-scale waves in the bottomside F-region at the onset of equatorial spread F, *Annales Geophysicae*, *26*(11), 3355–3364, doi:10.5194/angeo-26-3355-2008.

Tiwari, D., A. K. Patra, C. V. Devasia, R. Sridharan, N. Jyoti, K. S. Viswanathan, and K. S. V. Subbarao (2004), Radar observations of 8.3-m scale equatorial spread F irregularities over trivandrum, *Annales Geophysicae*, *22*(3), 911–922, doi: 10.5194/angeo-22-911-2004.

Woodman, R. F. (2009), Spread F an old equatorial aeronomy problem finally resolved?, *Annales Geophysicae*, *27*(5), 1915–1934, doi:10.5194/angeo-27-1915-2009.